

## Cleavage Fracture of Two Polystyrenes

### Synopsis

Suspension and bulk-polymerized commercial polystyrenes have been fractured by cleavage and the resulting surfaces examined by optical and scanning electron microscopy. The method of styrene polymerization was found to influence the initiation and propagation of fracture, probably owing to the differing amounts of insoluble impurities remaining in the polymer. Various new aspects of the fracture morphology are described, and measurements of craze thickness by scanning electron microscopy are compared with values calculated from optical interference fringes.

### INTRODUCTION

Recently, fairly comprehensive descriptions of fracture surfaces on Carinex (Shell Chemicals Limited suspension polystyrenes) have been provided by Murray and Hull<sup>1-6</sup> and Bird et al.<sup>7</sup> Prior to these, some published information was available.<sup>8,9</sup> All this work on fracture surface morphology of polystyrene employed tensile tests on materials manufactured by suspension polymerization. The present work differed in that a suspension and bulk polymerized polystyrene were studied. Cleavage techniques were used because they offered the possibility of much greater crack control than did tensile fracture.

### MATERIALS

Two polystyrenes were used: Carinex GP (Shell Chemicals Limited) suspension polymer,  $\bar{M}_w = 2.3 \times 10^5$ ,  $\bar{M}_n = 10.5 \times 10^4$ ; and Sternite 30 (Sterling Moulding Materials Limited) bulk polymer,  $\bar{M}_w = 2.4 \times 10^5$ ,  $\bar{M}_n = 2.5 \times 10^4$ . (Molecular weight data supplied by Shell Carrington Plastics Laboratory and Sterling Moulding Materials, Stalybridge.)

### EXPERIMENTAL METHODS

Substantially strain-free and orientation-free sheets of thickness 6.4 mm were compression molded from the two polystyrenes, and cleavage fracture test pieces were cut from them. During the molding, the polystyrenes were held at 200°C and 6 MN/mm<sup>2</sup> for 15 min to allow excess polystyrene to flash from the mold and for relaxation of the orientation introduced during flow in the mold. The resulting sheets were annealed at 87° ± 1°C and cooled to room temperature over about 10 hr to minimize frozen-in strain.

Cleavage fracture tests were carried out at 22° ± 1°C using two types of test piece. Some of the tests employed rectangular strips of the type described by Berry,<sup>10</sup> but the

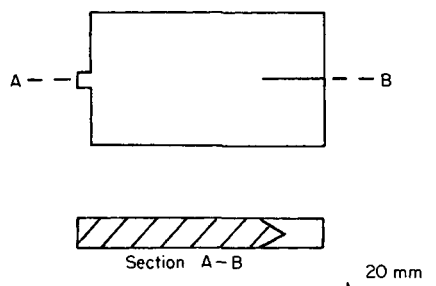


Fig. 1. Modified cleavage test piece.

majority of the observations employed a smaller cleavage test piece modified to provide some compression along the crack plane (Fig. 1). Both types of test piece resulted in apparently identical fracture surface features, but because of the differences in shape and method of straining each had particular advantages.

The modified test piece consisted of a rectangle measuring approximately 45 mm  $\times$  30 mm having a small, raised region at the middle of one short edge and a swallowtail sawcut starting opposite it at the middle of the other short edge. A sharp knife was drawn along the swallowtail sawcut in order to increase and localize the stress concentration. The test piece was subsequently fractured by driving a wedge into the sawcut using a hand-operated screw. This method of stressing combined with the test piece form offered more sensitive control of the crack propagation process, so that in Carinex GP polystyrene, the transition from slow fracture to fast fracture and vice versa could be produced at will. The small raised region directly opposite to the swallowtail sawcut localized along the centerline of the test piece the compressive stress set up by the wedge and thereby encouraged the formation of a very flat fracture surface suitable for optical microscopy. This test piece also had the advantage of being very simple to prepare.

After fracture, the samples were examined by optical microscopy and then gold-palladium coated before being studied in a Mark I Stereoscan (Cambridge Instruments Limited) scanning electron microscope.

## RESULTS AND DISCUSSION

### General Observations

Slow crack growth initiated very readily in the suspension polymer but not in the bulk polymer. In the latter, catastrophic fast fracture usually set in immediately as crack initiated. This difference is believed to occur because the suspension polymer contains many more sites for fracture initiation than does the bulk polymer. It is

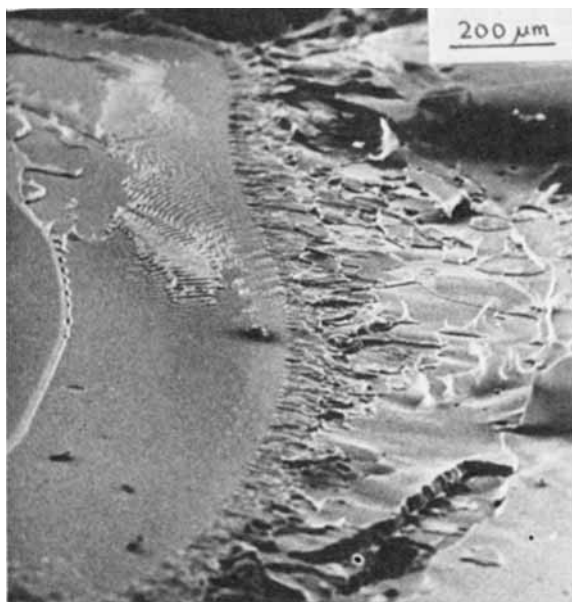


Fig. 2. Stereoscan micrograph of the region of a slow-fast transition on Sternite 30 (bulk polymer). Propagation from left.

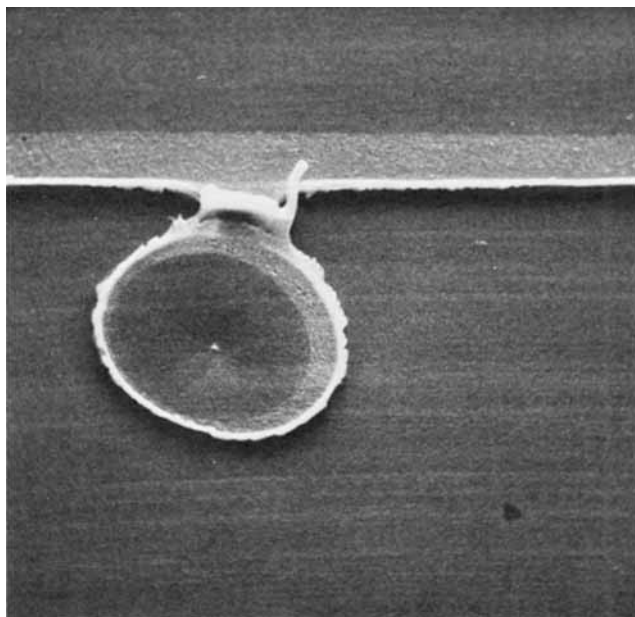


Fig. 3. Regions A and B on Sternite 30 showing a single secondary fracture in region B. Demonstrates thickness of craze layer. Propagation from the bottom.

necessary for one or more of these to be present at or close to the region of maximum stress at the tip of the swallowtail sawcut if slow controlled initiation and growth is to be achieved. If the nearest flaw is some distance from the point of maximum stress, a greater external stress must be applied to cause initiation; but immediately it is initiated, the crack grows into the maximum stress region and becomes unstable. Since there are relatively few initiation sites in the bulk polystyrene, it is rarely possible to initiate a slow crack in a cleavage test with this material.

The general features of the fracture surfaces were the same as have been reported by other workers,<sup>1-9</sup> i.e., there were three principal regions: region A corresponding to slow crack growth; region B corresponding to fast crack growth through the band of craze material which preceded the slow crack; and region C corresponding to fast crack growth through material which was substantially undeformed during the slow crack growth stage of fracture. Figure 2 shows these three regions on a bulk polymer fracture surface. A number of new observations were made:

1. A lesser number of secondary fractures were observed in the bulk polystyrene (generally  $10^{-2}$  to  $10^{-1}$  per  $\text{mm}^2$ ) compared to the suspension polystyrene (approx. 30 secondary fractures per  $\text{mm}^2$ .) This correlates with our suggestion<sup>11</sup> that secondary fractures initiate at impurity particles since in the bulk polymer no materials which are immiscible with the polymer are intentionally added during manufacture, whereas the suspension polymer contains soaps and suspension agents.

2. Direct observations were made of layers of craze material which had lifted from the fracture surface. This is shown in Figure 3, and for comparison the matching area of the other fracture surface is shown in Figure 4. The line across these micrographs is the position at which the onset of fast fracture occurred. In Figure 3, the lower half of the micrograph corresponds to slow crack growth (region A), and the upper half is region B. Fast fracture has occurred on both craze/polymer interfaces. The circular feature is a secondary fracture which formed during the slow growth stage of the main crack.

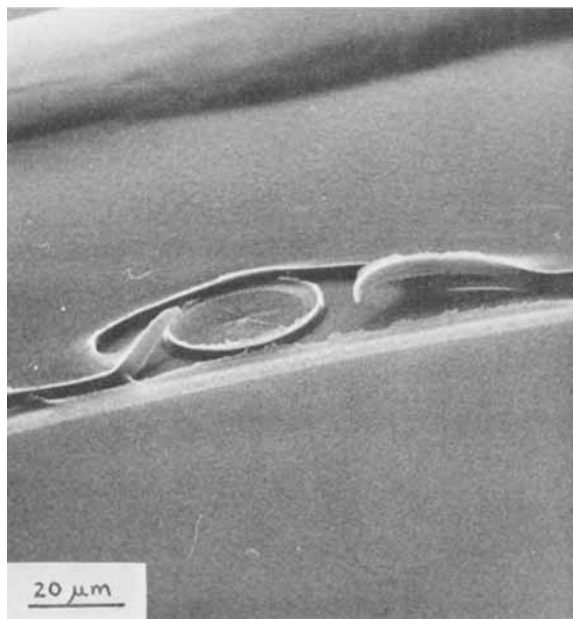


Fig. 4. Matching feature to Fig. 3 on the other fracture surface. Slow region A at top.

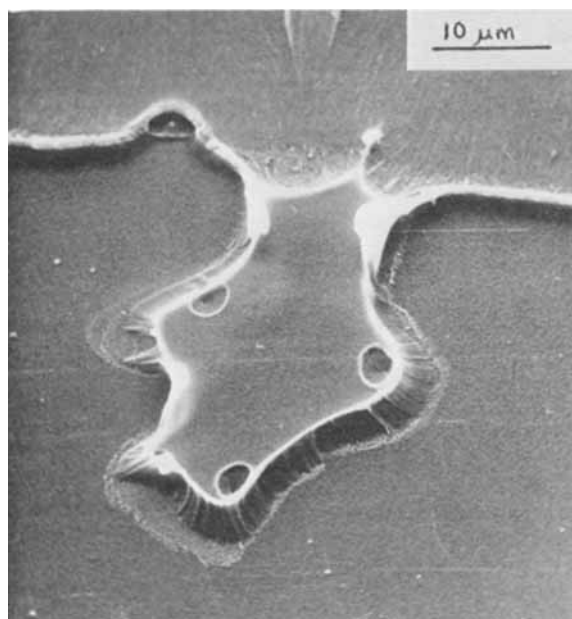


Fig. 5. Regions A and B on Carinex showing a change of crack plane caused by secondary fractures. Slow region at top.

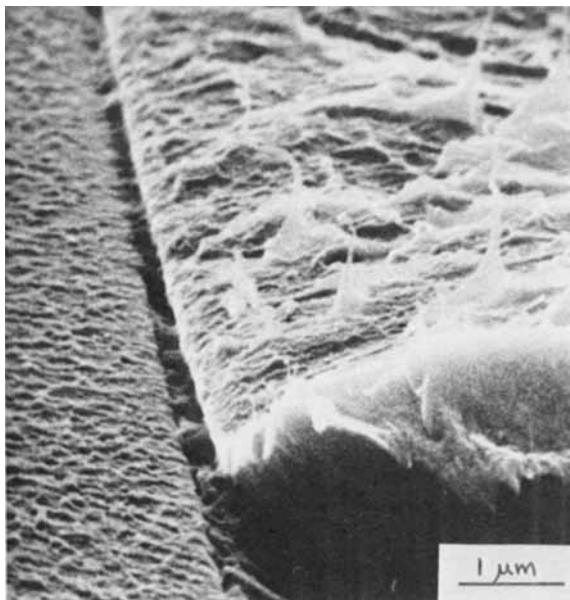


Fig. 6. Region B/region C boundary on Sternite 30. Note crack on boundary indicating bifurcation. Propagation from left.

3. In fracture region B, we observed that the choice of which craze/polymer interface the main crack followed was influenced by secondary cracks already present. The additive effect of the stress fields associated with the primary and secondary cracks causes the primary crack to follow preferentially the craze/polymer interface which is farther from the "plane" of the secondary crack. Actually, the surface of the secondary crack approximates a shallow cone with a small ( $0.1$  to  $1.0\ \mu\text{m}$  diameter) raised region at the center of the convex surface and a slightly larger depression at the center of the matching concave surface. The primary crack in region B moves to the other craze/polymer interface where secondary fractures are present which otherwise would be on the "wrong" side of the crack plane. An example is shown in Figure 5 where the primary crack has changed plane to accommodate three secondary fractures; but we have observed on many occasions a similar effect occurring, due to an isolated secondary fracture.

4. As the fast crack passes out of the band of craze which was formed during slow crack growth (i.e., from region B to C), frequently it bifurcates to form two cracks. An example of this is seen on Figure 6, where the dark line is a crack passing into the material.

5. We observed that, even at the highest crack speeds, a thin band of craze material formed ahead of the crack and a ductile surface structure resulted. This also can be seen in Figure 6 in region C to the right of the dark line.

#### MEASUREMENT OF CRAZE THICKNESS

Detail of mackerel pattern<sup>3</sup> on bulk polymer is shown in Figure 7. From this and similar micrographs, it was possible to measure directly the craze thickness across the fracture region B and compare the results with values calculated from optical interference fringes and Kambour's<sup>12</sup> figure of 1.33 for the refractive index of polystyrene craze.

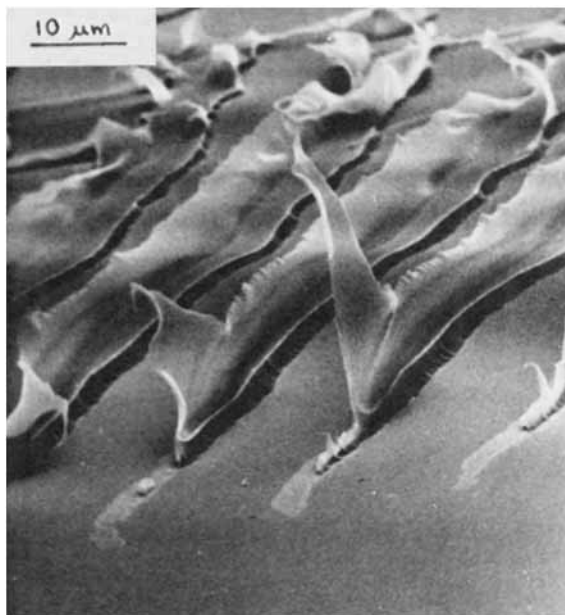


Fig. 7. Detail of mackerel structure showing the craze thickness decreasing across region B.

A typical region B on a bulk polystyrene cleavage surface was first photographed in reflected sodium light, and the thickness at various points of the craze layer was calculated from the interference fringes and wavelength of the light. The sample was then gold-palladium coated, and suitable regions where the fracture plane had changed from one craze boundary to the other within the area of the optical micrograph were found on the sample in the scanning electron microscope. The sample was then rotated until the angle of incidence of the primary electron beam was as large as possible, i.e., the angle between the electron beam and the fracture surface was small. Photographs were taken at high magnification to provide as accurate as possible an estimate of the craze thickness and subsequently at progressively lower magnifications in order to make a permanent record of the position on the fracture surface which had been examined.

In this way, the craze thickness was measured at six points and, after correction for the angle of incidence of the primary beam, the figures obtained were plotted together with the results calculated from the optical micrograph on Figure 8. It is estimated that each of the optically derived plots is accurate in position along the abscissa to within  $\pm 5$  microns, and the error along the ordinate depends only upon the accuracy of the refractive index figure (since the wavelength of the light is known very accurately). The stereoscan data are relatively inaccurate in the craze thickness (ordinate) direction, the error being variable but probably of the order of 5–10% on the worst results (those corresponding to areas near the middle of region B). In the abscissa direction, these plots are correct to within  $\pm 5$  microns.

From the plot in Figure 8 it is seen that the stereoscan data are in agreement with the optical data within the limits of accuracy of the experiments, but no accurate check on the refractive index is possible because the total error of the microscopic results is too great. The craze thickness decreases continuously from the boundary with region A but still is of measurable thickness at the boundary between regions B and C. This

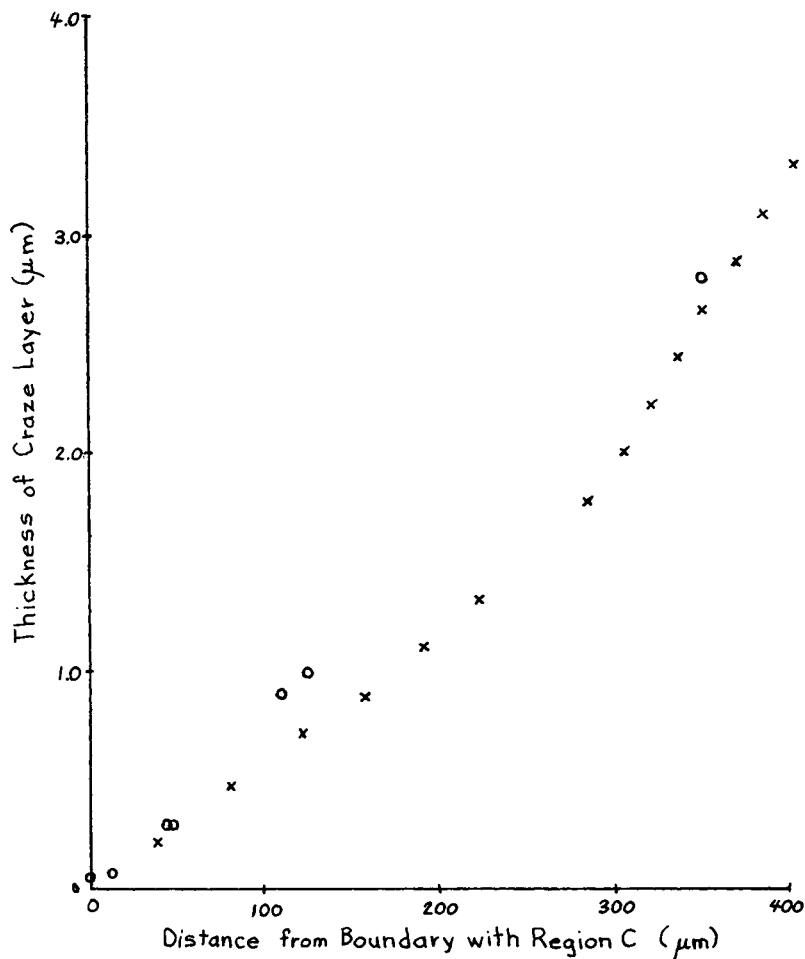


Fig. 8. Optical and SEM data on craze thickness in region B.

latter point was demonstrated by Figure 6, which showed this boundary on a bulk polymer sample, region B being on the left.

The authors are grateful to Mr. L. W. Turner for helpful discussions. This work was supported by the Ministry of Defence Procurement Executive.

#### References

1. J. Murray and D. Hull, *Polymer*, **10**, 451 (1969).
2. J. Murray and D. Hull, *J. Polym. Sci. B*, **8**, 159 (1970).
3. J. Murray and D. Hull, *J. Polym. Sci. A-2*, **8**, 583 (1970).
4. J. Murray and D. Hull, *J. Polym. Sci. A-2*, **8**, 1521 (1970).
5. D. Hull, *J. Mater. Sci.*, **5**, 357 (1970).
6. J. Murray and D. Hull, *J. Mater. Sci.*, **6**, 1277 (1971).
7. R. J. Bird, G. Rooney, and J. Mann, *Polymer*, **12**, 742 (1971).
8. R. J. Bird, J. Mann, G. Pogany, and G. Rooney, *Polymer*, **7**, 307 (1966).

9. R. N. Haward and I. Brough, *Polymer*, **10**, 736 (1969).
10. J. P. Berry, *J. Appl. Phys.*, **34**, 62 (1963).
11. B. L. Earl, R. J. Loneragan and M. Crook, *J. Mater. Sci.*, **8**, 370 (1973).
12. R. P. Kambour, *J. Polym. Sci.*, **A2**, 4159 (1964).

Yarsley Research Laboratories Limited  
Chessington, Surrey, England

Polytechnic of the South Bank,  
London, S.E.1, England

The Royal Armament Research and Development Establishment  
Fort Halstead, Kent, England

Received September 15, 1972  
Revised March 13, 1973

\* Present address: I.A.C.E., Sherborne House, Sherborne, Nr. Cheltenham, Glos.,  
England

B. L. EARL\*

M. CROOK

R. J. LONERAGAN  
J. H. T. JOHNS  
J. MARKHAM